Hydrol. Earth Syst. Sci. Discuss., doi:10.5194/hess-2016-493, 2016
Manuscript under review for journal Hydrol. Earth Syst. Sci.
Published: 5 October 2016

Hydrology and Earth System Sciences
Open Access
Discussions

Future shift of the relative roles of precipitation and temperature in controlling annual runoff in the conterminous United States

Kai Duan[1], Ge Sun[2*], Steven G. McNulty[2], Peter V. Caldwell[3], Erika C. Cohen[2], Shanlei Sun[4], Heather D. Aldridge[5], Decheng Zhou[4], Liangxia Zhang[4], and Yang Zhang[1]

[1] Department of Marine, Earth, and Atmospheric Sciences, North Carolina State University, Raleigh, NC, USA

[2] Eastern Forest Environmental Threat Assessment Center, USDA Forest Service, Raleigh, NC, USA

[3] Coweeta Hydrologic Laboratory, USDA Forest Service, Otto, NC, USA

[4] Key Laboratory of Meteorological Disaster of Ministry of Education, Nanjing University of Information Science & Technology, Nanjing, Jiangsu, China

[5] State Climate Office of North Carolina, North Carolina State University, Raleigh, NC, USA

Corresponding author: Ge Sun (gesun@fs.fed.us)

Hydrol. Earth Syst. Sci. Discuss., doi:10.5194/hess-2016-493, 2016
Manuscript under review for journal Hydrol. Earth Syst. Sci.
Published: 5 October 2016

Hydrology and Earth System Sciences
Open Access
Discussions

Abstract Precipitation and temperature are the two key climatic variables that control the hydrological cycle and water availability for humans. This study examines the potential shift of the relative roles of precipitation and temperature in controlling annual runoff in the conterminous United States (CONUS), using a water-centric ecohydrological model driven with historical records and climate scenarios constructed from 20 CMIP5 (Coupled Model Intercomparison Project Phase 5) climate models. The results suggest that precipitation has been the primary control of runoff variability and trend during the latest decades. However, the influence of temperature is projected to increase in a continued warming future in the 21st century. Despite considerable uncertainty and regional diversity, the multi-model ensemble reveals a high degree of consistency in the general increasing trend of both precipitation and temperature in the future, imposing positive and negative effects on annual runoff, respectively. The magnitude of temperature effect tends to exceed that of precipitation, and thus leads to an overall decrease of 8~30 mm yr^{-1} (3%~11%) runoff by 2100. Overall, temperature and precipitation changes are expected to contribute to runoff change by 58%~65% and 31%~39% separately, indicating that the role of rising temperature may outweigh that of precipitation in the later part of the 21st century. Across the CONUS, runoff decrease and increase in 34%~52% and 11%~12% of the land area are expected to be dominated by long-term changes in temperature and precipitation, respectively. We found that the vast croplands and grasslands across the central and forests in the northwestern regions might be particularly vulnerable to water supply decline caused by the changing climate.

Hydrol. Earth Syst. Sci. Discuss., doi:10.5194/hess-2016-493, 2016
Manuscript under review for journal Hydrol. Earth Syst. Sci.
Published: 5 October 2016

1 Introduction

Precipitation and temperature are the two key climatic variables that control land water balances and thus control water availability for both ecosystem and humans (Lutz et al., 2014; Milly et al., 2005; Piao et al., 2010; Seager et al., 2013). Changes in temperature interact with changes in precipitation and cause profound shifts in hydrologic paradigms, such as snowpack melting and accumulation (Barnett et al., 2005; Zhang et al., 2015), intensification of hydrologic cycle (Creed et al., 2015; Davis et al., 2015), precipitation partitioning (Duan et al., 2016b; Zhou et al., 2015), extreme floods and droughts (Duan and Mei, 2014a; Duan et al., 2016a; Trenberth et al., 2014), and can lead to hydrological 'nonstationarity' (Milly et al., 2008).

Surface and subsurface (shallow aquifers) runoff is the critical source of fresh water that human populations sustainably have access to (Vörösmarty et al., 2000). The impacts of temperature and precipitation changes on the magnitude and variability of runoff (Arnell and Gosling, 2013; Ficklin et al., 2009; Nash and Gleick, 1991; Vano et al., 2012) have drawn particular attention due to its importance for water supplies. Future changes in precipitation, evaporation, and plant water use are direct driving forces of runoff generation. Global warming alters both precipitation and the partitioning of precipitation into evapotranspiration (Et) and runoff since a warmer climate generally provides more energy for water fluxes between the land and the atmosphere. Although an increase in precipitation may cause increase in both Et and runoff, the enhanced evaporative demand can results in decrease in runoff efficiency (ratio of runoff to precipitation) (McCabe and Wolock, 2016). Both

Hydrol. Earth Syst. Sci. Discuss., doi:10.5194/hess-2016-493, 2016
Manuscript under review for journal Hydrol. Earth Syst. Sci.
Published: 5 October 2016

Hydrology and Earth System Sciences Discussions

observation and simulation studies in the U.S. suggest that higher Et induced by rising temperature is unlikely to be counterbalanced by the increase in precipitation and lead to less runoff at large scales (Duan et al., 2016b; Jackson et al., 2005). Conversely, global warming may also cause precipitation decrease in some regions and exacerbate the effects of temperature on runoff change.

Several studies have examined the relative contributions of historical changes in precipitation and temperature to runoff variation at watershed (Karl and Riebsame, 1989), regional (Gupta et al., 2015; Ryberg et al., 2014), and continental (McCabe and Wolock, 2011) levels across the CONUS. These studies all agree that precipitation, instead of temperature, explains most of the long-term change and variability in runoff during the past century. However, the role of temperature may become more substantial under the continued warming climate. According to the Parameter-elevation Relationships on Independent Slopes Model (PRISM) dataset (http://prism.oregonstate.edu/) (Daly et al., 2008), the rate of decadal change over the CONUS reaches -0.03~+0.28 °C since 1960s. The rate of warming is likely to accelerate under intermediate or high emission scenarios and increase the pressure of water scarcity in most regions in this century (IPCC, 2014; Schewe et al., 2014). In addition, future change in climate is projected to vary spatiotemporally in both direction and magnitude in the CONUS (Mearns et al., 2012), thus sensitivity of water budget to climate change may be discrepant across time and space. Although the possible underestimation of the influence of temperature in altering regional water resources has been discussed in recent researches (e.g. Woodhouse et al.,

Hydrol. Earth Syst. Sci. Discuss., doi:10.5194/hess-2016-493, 2016
Manuscript under review for journal Hydrol. Earth Syst. Sci.
Published: 5 October 2016

Hydrology and Earth System Sciences
Open Access
Discussions

2016), a comprehensive evaluation of the relative roles of precipitation and temperature under different climate backgrounds and land-cover compositions is still lacking.

The question we aim to address is: to what extent, if any, will the relative roles of precipitation and temperature in controlling runoff shift if future climate changes follow the projections of the state-of-the-art climate models? In another word, how will the roles of the climate factors shift if climate change in the rest of this century does not follow the tendencies documented in the recent decades? Specifically, the objectives of this study are to (1) quantify the contributions of changes in precipitation and temperature to annual runoff variation by testing both historical observations and Global Climate Model (GCM) projections, and (2) investigate the spatial pattern of runoff change and its dominant driving factors across the CONUS. In the remainder of the paper, we first describe the methodology of runoff simulation and sensitivity assessment, and the hydro-climatic datasets used, followed by the results. Then, the advantages, limitations, and implications of this study are discussed and the conclusions are drawn.

2 Methods

2.1 Runoff modeling

The runoff responses to climate change and variability are modeled with the Water Supply Stress Index model (WaSSI) for over 82,000 12-digit Hydrologic Unit Code (HUC-12) watersheds (http://water.usgs.gov/GIS/huc.html) across the CONUS. WaSSI is a water-centric ecohydrological model that simulates the land-cover

Hydrol. Earth Syst. Sci. Discuss., doi:10.5194/hess-2016-493, 2016
Manuscript under review for journal Hydrol. Earth Syst. Sci.
Published: 5 October 2016

specific water and carbon cycles (Caldwell et al., 2012; Sun et al., 2011b). The model incorporates several mathematical sub-models to describe monthly hydrologic processes from precipitation input to streamflow routing. A conceptual snow sub-model (McCabe and Markstrom, 2007) is used to partition the total precipitation into rainfall and snowfall, and to estimate snowpack melt/accumulation and snow water equivalent with concern of the mean elevation, latitude, and air temperature in the watershed. Et is calculated with an ecosystem Et model developed from the empirical relationships between Et and precipitation, Hamon's potential evapotranspiration (PET), and leaf area index (LAI) (Sun et al., 2011a; Sun et al., 2011b). These functions were established for 10 different land-cover classes independently to account for the different water demand within different vegetation, ranging from cropland, deciduous forest, evergreen forest, mixed forest, grassland, shrubland, wetland, open water, urban area, to barren land. Then, this Et estimation is further constrained by soil water availability, which is simulated using the algorithms of Sacramento Soil Moisture Accounting model (SAC-SMA) (Burnash, 1995), as well as the processes of infiltration and runoff generation at monthly basis.

Necessary inputs for WaSSI include monthly precipitation, air temperature, LAI, and land-cover composition. In this study, the spatial distribution of LAI and the 10 land-cover classes (Fig. 1a) were assumed to be static over time. Monthly climate inputs were first scaled to HUC-12 watersheds and then used to drive the model. All of the water balance components were calculated independently for each land cover class within each watershed, and then aggregated to compute the monthly means of

Hydrol. Earth Syst. Sci. Discuss., doi:10.5194/hess-2016-493, 2016
Manuscript under review for journal Hydrol. Earth Syst. Sci.
Published: 5 October 2016

Hydrology and Earth System Sciences
Discussions

the watershed. The model parameters were acquired from several previous studies, including: (1) The parameters of snow sub-model were estimated for each Water Resource Region (WRR, i.e., 2-digit HUC watershed) (Fig. 1b) by comparing regional monthly mean snow water equivalent to remotely sensed values from the Snow Data Assimilation System (Caldwell et al., 2012; McCabe and Markstrom, 2007). (2) The parameters of Et sub-model were estimated by empirical relationships derived from multisite eddy covariance or sapflow measurements (Sun et al., 2011a; Sun et al., 2011b). (3) SAC-SMA parameters used to drive the soil water balance model were taken from the State Soil Geographic Database (http://soildatamart.nrcs.usda.gov) that was established based on physical soil characteristics over the CONUS (Anderson et al., 2006; Koren et al., 2003).

The WaSSI model has been validated against observations at U.S. Geological Survey (USGS) gauged sites at the levels of both 8-digit (Caldwell et al., 2012) and 12-digit HUC watersheds (Sun et al., 2015b). We here verify the model performance at WRR and continental scales to complement to previous validations. The simulated annual runoff, driven by monthly precipitation and temperature from the PRISM dataset, was compared against the USGS measurements over the entire CONUS (Fig. 2a&2c) and in the 18 WRRs (Fig. 2b&2d) during 1961-2010. Despite a slight overestimation of minimums, WaSSI shows reliable accuracy in capturing annual runoff at both CONUS and WRR scales, with R-square statistic reaching 0.91 and 0.95, and Root Mean Squared Error (RMSE) limited to 29 and 55 mm yr^{-1}, respectively.

Hydrol. Earth Syst. Sci. Discuss., doi:10.5194/hess-2016-493, 2016
Manuscript under review for journal Hydrol. Earth Syst. Sci.
Published: 5 October 2016

2.2 Quantifying the roles of precipitation and temperature

Large-scale water balance can be described as precipitation (P) and changes in the hydrologically connected snowpack (ΔSp) equal ET plus runoff (R):

$$P + \Delta Sp = Et + R \quad (1)$$

While P is the primary water input, changing temperature (T) interacts with changing P and affects R by altering the melt/accumulation of snowpack and controlling Et with the constraints of vegetation and soil moisture.

Here we developed a simple approach of sensitivity test to examine the relative roles of precipitation and temperature in runoff variation. The total effects of P and T changes on R (ΔR) are divided into three components:

$$\Delta R = \Delta R_P + \Delta R_T + \Delta R_{P\&T} \quad (2)$$

where ΔR represents the combination of the independent effects of P (ΔR_P), the independent effects of T (ΔR_T), and the effects of interactions between changes in P and T ($\Delta R_{P\&T}$). ΔR is quantified by the total changes (%) in R from pre-change period (t_1) to post-change period (t_2) as $R\{P(t_2),T(t_2)\}-R\{P(t_1),T(t_1)\}$; while ΔR_P (or ΔR_T) is estimated by the R change (%) driven by P (or T) change only, with the assumption that the other driving factor is stagnant from t_1 to t_2, as $R\{P(t_2),T(t_1)\}-R\{P(t_1),T(t_1)\}$ (or $R\{P(t_1),T(t_2)\}-R\{P(t_1),T(t_1)\}$). $\Delta R_{P\&T}$ is calculated as the difference between ΔR and ΔR_P+ΔR_T, representing the changes in R that cannot be accounted for by ΔR_P or ΔR_T.

The three components above may cause either positive or negative effects on R. Their contributions to runoff change are quantified by the relative weights of their

Hydrol. Earth Syst. Sci. Discuss., doi:10.5194/hess-2016-493, 2016
Manuscript under review for journal Hydrol. Earth Syst. Sci.
Published: 5 October 2016

impact. For instance, the contribution (%) of P can be calculated as

$$Con\ (P) = 100 \times |\Delta R_P| \ / \ (\ |\Delta R_P| + |\Delta R_T| + |\Delta R_{P\&T}| \ ) \tag{3}$$

2.3 Modeling experiments

2.3.1 Detecting of observed historical changes

Historical changes in precipitation, temperature, and their effects on runoff were tested using monthly precipitation and temperature records from the PRISM dataset spanning from January 1960 to December 2010. The original data on 4 km × 4 km grid cells was scaled to HUC-12 watersheds for modeling monthly runoff. Given to the significant spatial and temporal variability in runoff trend across the CONUS (Gupta et al., 2015; Mauget, 2003; McCabe and Wolock, 2002; McCabe and Wolock, 2011), a consistent breakpoint is statistically unavailable for our analysis at different spatial scales. We hereby take 1985 as the breakpoint year for all the watersheds and divide the PRISM dataset into two 25-year periods. The historical changes in runoff were evaluated as the difference between the multi-year mean annual values in the pre-change period 1961-1985 and the post-change period 1986-2010, while the data in 1960 was discarded after warming up the model. Although the selection of different breakpoints may lead to deviations in the examination of the roles of precipitation and temperature, the analysis can provide a comparable benchmark for exploring the shifts in future scenarios at multi-decadal scale.

2.3.2 Detecting of potential changes in future

Projections of monthly precipitation and temperature derived from 20 GCMs of the fifth phase of the Coupled Model Inter-comparison Project (CMIP5) for both historical forcings and future Representative Concentration Pathways (RCPs) were used to test the potential runoff changes in future. RCP4.5 and RCP8.5 were adopted as representatives of the intermediate and high emission scenarios respectively, which correspond to radiative forcing of approximately 4.5 W m^{-2} and 8.5 W m^{-2} in 2100 (equivalent to 650 ppm and 1370 ppm CO_2) (IPCC, 2014; Moss et al., 2010). The raw output of GCM simulations were downscaled using the Multivariate Adaptive Constructed Analogs method (MACA) (Abatzoglou and Brown, 2012) to fill the spatial gaps and remove the systematic biases of the GCMs, with the LIVNEH observational dataset (Livneh et al., 2013) as training data. The datasets of statistically downscaled output for the CONUS (the MACAv2-LIVNEH) are available at http://maca.northwestknowledge.net/.

To evaluate the runoff responses to various changes in future climates, we extracted four experiments of 30-year monthly precipitation and temperature from each GCM output, including: (i) RCP4.5/2030s (S1) — 1st future period 2020-2049 under RCP4.5 scenario, (ii) RCP4.5/2080s (S2) — 2nd future period 2070-2099 under RCP4.5 scenario, (iii) RCP8.5/2030s (S3) — 1st future period 2020-2049 under RCP8.5 scenario, and (iv) RCP8.5/2080s (S4) — 2nd future period 2070-2099 under RCP8.5 scenario. These four future scenarios cover two different time periods (2030s and 2080s) as the post-change periods, and were tested against a pre-change period of 1970-1999 that represents the current, or baseline level. This large set of simulations (Table 1) was pooled to enable a robust quantification of the major uncertainties from GCM structure and emission scenario. The projected changes in mean annual precipitation and temperature in the CONUS varies between -70 ~ +87 mm yr^{-1} and +0.8 ~ +6.9 °C among the climate models and scenarios. The inter-GCM ranges suggest a general increase in both precipitation and temperature, with the median change reaching +15 ~ +31 mm yr^{-1} and +1.8 ~ +5.3 ℃ in the four future scenarios, respectively.

3. Results

3.1 Changes in runoff in future climates

Changes in mean annual runoff under future climate change scenarios vary among HUC-12 watersheds (Fig. 3) and WRRs (Fig. 4) across the CONUS. The multi-model average changes (Fig. 3) span from less than -50% (decrease) to over +100% (increase). While modest decreases smaller than 20% are projected to occur across most part of the CONUS from northwest to southeast, extreme decreases are scattered across the western half of the country in WRR10 (Missouri), WRR11 (Arkansas-White-Red), and WRR17 (Pacific Northwest). On the other hand, increase can be mainly found along the eastern coast from WRR1 (New England) to WRR3 (South Atlantic-Gulf), and in the southeastern regions across WRR13 (Rio Grande), WRR15 (Lower Colorado), and WRR18 (California). Increases are especially extreme (e.g., >500%) in the borders of WRR15 and WRR18. However, this may be caused by the incapability of GCMs in reproducing the low precipitation amounts in these extremely dry watersheds. Although the general spatial pattern appears similar in the four scenarios, there is an evident expansion of the areas showing either extreme increasing or decreasing trend from 2030s to 2080s under both RCP4.5 (Fig. 3a-3b) and RCP8.5 (Fig. 3c-3d) scenarios.

The large variability in regional changes in runoff (Fig. 4) indicates considerable uncertainties from GCM structure. In most cases, the uncertainty range is limited to -40% ~ +20%, showing both positive and negative changing signals. However, the distributions of the median lines and Inter-Quartile Ranges (IQRs) suggest a hydrologically drier future in most of the WRRs. A large decrease can be seen in WRR7~11, WRR14 (Upper Colorado), and WRR16 (Great Basin), where the IQRs stay below the zero line in all the scenarios. WRR1 is the only region that shows a strong increasing trend, especially in S1~S3 scenarios. Positive median value can also be occasionally found in WRR2~3, WRR5 (Ohio), WRR6 (Tennessee), and WRR18, with the IQRs straddling the zero line. Generally, the uncertainty ranges tend to increase from 2030s to 2080s under both RCPs, and reach a particularly high level under S4 scenario (RCP8.5/2080s). There is a noticeable consistency in this pattern that the GCMs agree more on the simulations in 2030s while the uncertainty aggregates over time toward 2080s, which implies the limitation of the state-of-the-art GCMs in addressing predictions of further future.

The aggregated effects of precipitation (P), temperature (T), interactions between P and T ($P\&T$), and their combination (Total) on runoff over the entire CONUS in the future are illustrated in Fig. 5a. P and T are projected to cause divergent changes in R. The median values show that mean annual runoff under independent P effect is expected to increase by 17 mm yr^{-1} (6%) in 2030s and 27 mm yr^{-1} (10%) in 2080s under RCP4.5, and by 22 (8%) and 34 (12%) mm yr^{-1} at the same time under

Hydrol. Earth Syst. Sci. Discuss., doi:10.5194/hess-2016-493, 2016
Manuscript under review for journal Hydrol. Earth Syst. Sci.
Published: 5 October 2016

RCP8.5 (i.e., ΔR_P). In contrast, the independent effects of T reach -28 (-10%), -45 (-17%), -31 (-11%), and -74 (-27%) mm yr^{-1} in the scenarios S1~S4 (i.e., ΔR_T). In general, while the effects of $P\&T$ are minimal, the negative effect of rising T exceeds the positive effect of increasing P, and leads to extensive decreases in runoff by -10 (-4%), -21 (-8%), -8 (-3%), and -30 (-11%) mm yr^{-1} in the four scenarios, respectively. The variation of uncertainty range follows the same pattern of expanding from 2030s to 2080s, however, the IQRs of 'Total' effects remain negative and suggest reliable decreasing trend in runoff. It is worth noticing that the uncertainty range of P effect constantly surpasses that of T effect. Especially in S4 scenario, the multi-model result of P effect ranges from -10% to 26%, and the IQR also reaches the highest level (13%). It suggests that uncertainty in precipitation projection is still the largest contributor to the uncertainty in runoff simulations.

3.2 Relative contributions of *P* and *T*

Table 2 summarizes the contributions of P, T, and $P\&T$ to runoff change in the historical period (from 1961-1985 to 1986-2010) and the future scenarios (from baseline to S1~S4) in 18 WRRs and CONUS. Despite different methodologies, the result of the latest decades is similar to a previous evaluation performed by McCabe and Wolock (2011) that P plays a dominating role with a contribution over 99% in all of the 18 regions. However, the changes in T in the future scenarios (+1.4 ~ +6.2 °C) are expected to be much larger than that in the latest decades (+0.2 ~ +0.7 °C), causing more significant increases in Et (from -3% ~ +5% to -0.5% ~ +30%) that cannot be fully offset by the potential increases in P (see the details of

Hydrol. Earth Syst. Sci. Discuss., doi:10.5194/hess-2016-493, 2016
Manuscript under review for journal Hydrol. Earth Syst. Sci.
Published: 5 October 2016

regional changes in P, T, PET, Et and R in Table S1~S5).

The multi-model means of the 20 GCMs (Table 2) suggest that T will become the overwhelming driver in most of the regions in the future. In contrast, P continues to be the largest contributor in WRR1 (S1~S3), WRR12 (Texas-Gulf) (S1), and WRR18 (S1~S4) in various scenarios. The contribution of $P\&T$ varies between 1%~17% among regions with a continental average of 3%~6%, indicating that the independent effects of P and T can explain nearly all of the runoff variation.

The difference between the contributions of P and T is projected to spread a wide range (3%~38%) among the regions and scenarios. Due to the inconsistency in the results derived from distinct GCMs, a close difference in the multi-model means (e.g., 48% and 51%) may make the recognition of larger contributor dubious. To examine the statistical significance of these differences, we assumed that the differences of P or T contribution derived from the 20 GCMs are from a continuous distribution, and used the Wilcoxon signed-rank test method (Gibbons and Chakraborti, 2011) to test if it converges to zero. The test results (Table 2) suggest that T contribution is significantly larger (at the 5% significance level) over the entire CONUS and in WRR7, 9~11, 14, and 16 in all the future scenarios. Meanwhile, insignificance can be constantly found in the northeast (WRR1~2), south (WRR12), and southwest (WRR15,18), suggesting that the contributions of P and T are expected to be equivalently important, or at least close in these regions.

For the entire CONUS (Fig. 5b), the median contribution of T rises from 60% in 2030s to 63% in 2080s under RCP4.5, and from 58% in 2030s to 65% in 2080s under RCP8.5. Meanwhile, the median contribution of *P* reaches 34%, 35%, 39%, and 31% under the four scenarios, respectively. This result is consistent with the comparison of separate effects of *P*, *T*, and *P&T* on runoff, but it should be kept in mind that significant uncertainty is involved due to the highly diverse projections of the changes. In general, both the contributions of *P* and *T* span a large uncertainty range, with the IQRs varying between 13%~23% and 15%~23%.

3.3 Spatial distributions of the driving factors

To further investigate the spatial pattern of the roles of *P* and *T* across the CONUS, we divide all the HUC-12 watersheds into three classes according to the dominant driving factors: (1) *P*-dominant, if the multi-model mean contribution of *P* change (refered to as *MCP*) is larger than 50%, and the difference between the contributions of *P* and *T* is significant (passing the the Wilcoxon signed-rank test); (2) *T*-dominant, if the mean contribution of *T* change (refered to as *MCT*) is larger than 50%, and the difference between the contributions of *P* and *T* is significant; (3) Non-dominant, if both *MCP* and *MCT* are less than 50%, or the difference is not significant. We find that the spatial distributions of *P*-dominant and *T*-dominant areas (Fig. 6 and Table 3) coincide with the areas with increasing and decreasing trends in *R* (i.e., ΔR) (Fig. 3), respectively. The areas with a generally larger *T* effect ($MCT > MCP$) are projected to cover a major part of the country, and significant dominance of *T* effect can be found in the central (WRR5, 7, 9~11) and northwest (WRR14, 16, 17) of the CONUS in all the future scenarios. The *P* effect prevails ($MCP > MCT$) in a considerable portion of watersheds in the Atlantic coast (WRR1~3), Pacific coast

Hydrol. Earth Syst. Sci. Discuss., doi:10.5194/hess-2016-493, 2016
Manuscript under review for journal Hydrol. Earth Syst. Sci.
Published: 5 October 2016

Hydrology and Earth System Sciences
Open Access
Discussions

(WRR17~18), and southwest (WRR13~16), and results in a hydrologically wetter future in these areas. Significant *P*-dominant areas are expected to cover up to 70% of the southwest (WRR13, 15, 18) and the northern part of WRR1.

In summary, 34%~52% and 11%~12% of the land area are expected to be *T*-dominant and *P*-dominant in the future climates, respectively (Table 3). Although the total proportion of area under *P* dominance is rather stable over time, *T*-dominant area is projected to increase from 36% to 47% under RCP4.5, and from 34% to 52% under RCP8.5 along with the rise of temperature. At regional level, a directional change can be seen in the eastern and western regions of the country between the two future periods. Expansion of the *T*-dominant area, as well as the shrinkage of *P*-dominant area, is projected to occur from 2030s to 2080s in the eastern CONUS across WRR1~WWR5. A considerable rise of *P*-dominant area, in the meantime, can be found in the western CONUS across WRR13~WRR18.

4. Discussion

4.1 Spatial patterns

The coherence in the spatial dynamics of runoff trend and corresponding dominant climatic drivers shows a rough general pattern: *P* change dominates *R* increase while *T* change dominates *R* decrease. However, it should be interpreted with caution. We simplified the criteria of dominant driver as the multi-model averaged contribution exceeding 50%, so the relative importance of the dominant driver may differ significantly among regions. In the *P*-dominant regions including WRR1, WRR15, and WRR18 (Fig. 6), the difference between the contributions of *P* and *T* (Table 3) is

Hydrol. Earth Syst. Sci. Discuss., doi:10.5194/hess-2016-493, 2016
Manuscript under review for journal Hydrol. Earth Syst. Sci.
Published: 5 October 2016

Hydrology and Earth System Sciences Open Access Discussions

relatively smaller than that in the *T*-dominant regions across central CONUS. At HUC-12 scale, this pattern does not hold true in all the watersheds due to the nonlinear complexity of *R* response to climate change at various time scales, as well as the influence of other watershed characteristics (e.g., topography, land-cover, land-use, soil property). For example, slight decreases in *P* and yet increases in *R* are projected in south Texas due to the alteration of inner-annual climate variability; the role of temperature can be more positive in regions where water availability is dominated by snow melting (Barnett et al., 2005; Lutz et al., 2014). Also, local runoff can be disturbed by other factors, such as solar dimming, land-cover evolution, and the direct effects of atmospheric composition on transpiration (Gedney et al., 2006; Zhang et al., 2015; Zhang et al., 2001).

Nevertheless, this pattern explains the major characteristics of large-scale inter-relationships among changing *P*, *T*, and *R* despite the large geographic differences. Overall, the projections of the GCMs show a high agreement on the increases in both *P* and *T*. As the control of watershed water supply, *P* continues to be an important factor and generally shows positive effects on *R*. On the other hand, increasing *T* will impact the hydrological cycle by enhancing Et and suppressing *R*. Driven by the combined effects, *R* is expected to respond to climate change with an overall decreasing trend as well as high spatial variability.

4.2 The role of land cover

Land cover, LAI, and soil are the key controls on catchment water balance and runoff sensitivity to climate change (Bosch and Hewlett, 1982; Cheng et al., 2014;

Zhang et al., 2001). This study specifically focuses on evaluating the separate and combined effects of changing precipitation and temperature on runoff within a static environmental background. We do not consider the potential evolution of land cover and its interactions with water balance. We make no explicit tabulation of the impact of land cover/land use on the runoff responses to climate change, but we do incorporate it as a key factor by estimating Et with a set of functions of *P*, *T*, LAI, and soil moisture capacity and deficit. One basic assumption of our ecohydrological simulation is that larger LAI leads to higher Et when water supply is sufficient. In line with this assumption, the overall *T* effect on *R* projected in forests and croplands is slightly larger than that in urban and barren lands due to the higher Et (see Table S6 for the multi-model average contributions of *P*, *T*, and *P&T* to *R* changes in 10 land cover classes). Across the land cover classes, the uncertainty ranges of independent contributions of *P* (26%-40%) and *T* (53%-66%) are relatively small compared to the ranges across WRRs (26%-56% and 38%-67%). This may be because the discrepancy across different land covers is largely offset by the different climate backgrounds across the country. Evaluation of future land cover change and its impact on runoff is out of the scope of this study. However, our results imply that the potential impact of land cover change might not be large enough to alter the relative significance of *P* and *T* in controlling future continental water availability.

4.3 Implications for water and land management

Our results have important implications for water and land management across the CONUS. Water resource planning may need to prepare different management

Hydrol. Earth Syst. Sci. Discuss., doi:10.5194/hess-2016-493, 2016
Manuscript under review for journal Hydrol. Earth Syst. Sci.
Published: 5 October 2016

strategies for *P*-dominant and *T*-dominant areas that have contrasting future hydrological conditions. Additional water storage such as reservoirs and flood prevention measures may be needed in regions expecting more runoff, while inter-basin water transfer, improving water use efficiency, and other water conservation measures such as rain harvesting, and waste water recycling should be implemented for areas expecting water shortages. In addition, the vast croplands across central U.S. (WRR5, 7, 9~10) are likely to be threatened by rising air temperature and diminishing water availability for irrigation and food production. Adaptations in cropping systems and irrigation strategy are needed to secure food supply and increase resiliency to drought and changing climate (Challinor et al., 2014; Teixeira et al., 2013). The drier and hotter conditions may also result in increasing water stress, higher risks of tree insects and disease outbreaks, and catastrophic wildfires in forests (Dale et al., 2001) (e.g., National Forests in WRR16~18) and grasslands (e.g., in WRR10~11). Innovative land management practices such as forest thinning and fuel management, irrigation, and planting drought-tolerant species are vital to minimize the potential risk and vulnerability to climate change and reduce the threats to ecosystems and society (Grant et al., 2013; Sun et al., 2015a; Vose et al., 2016).

4.4 Sources of uncertainty

Considerable uncertainty lies in the projection of future changes in precipitation and temperature from the 20 GCMs. The uncertainty ranges under both RCP4.5 and RCP8.5 show significant expansions over time from 2030s to 2080s. In particular, the large uncertainty in predicting future precipitation may substantially compromise the reliability in evaluating either runoff change or precipitation and temperature's roles (Karl and Riebsame, 1989; Piao et al., 2010). For example, 16 out of 20 GCMs agree that *T* will be a larger contributor than *P* in S1 scenario, while there are still four models suggesting the opposite. The results allow us to draw some robust conclusions on the general patterns, but uncertainties are large and varied differently across space and time. Also, a limitation of this study is that we did not incorporate other sources of uncertainty, such as the methodology of downscaling (Chen et al., 2011; Duan and Mei, 2014b), structure and parameters of hydrologic model (Jung et al., 2012), and the estimation of future PET (Bae et al., 2011; Milly and Dunne, 2016). Although the selection of GCM and emission scenario are most likely to be the largest sources of uncertainty in hydro-climatic modeling (Duan and Mei, 2014a; Kay et al., 2009; Wilby and Harris, 2006), the other sources may also have influence on the results to different extents. The roles of uncertainties from different sources can be particularly equivocal when investigating seasonal/monthly variability and extreme events (Bae et al., 2011; Bosshard et al., 2013; Giuntoli et al., 2015; Kay et al., 2009).

5. Conclusions

This study evaluates the relative roles of precipitation and temperature in annual runoff variation across the CONUS based on a large ensemble of simulations using data from both historical measurements and GCMs projections. Despite the large uncertainty and spatial variability involved, two robust conclusions can be drawn at the CONUS and regional scales on multi-decadal basis. First, the projections from 20 GCMs suggest a high degree of consistency in the overall increasing trends in both precipitation and temperature, which leads to positive and negative effects on runoff when considered separately. The magnitude of warming effect is projected to exceed that of increase in precipitation. The estimated contribution of temperature change (58%~65%) also outweighs that of precipitation change (31%~39%) and results in up to 30 mm yr^{-1} (11%) decrease in the annual runoff over the entire CONUS. Second, the spatial patterns of watershed runoff change reveal that long-term changes in temperature and precipitation are likely to be the dominant driving factors of runoff change in 34%~52% and 11%~12% of the land area, respectively. Temperature change tends to suppress runoff in a major part of the country, especially in the central (WRR5, 7, 9~11) and northwest (WRR14, 16, 17) of the CONUS. Conversely, precipitation change is projected to be the dominant factor in a considerable portion of watersheds across the Atlantic coast (WRR1~3) and the southwest (WRR13~18). As both temperature and precipitation increase over time (2030s~2080s) in the rest of the 21st century, water availability in more areas are expected to be dominated by temperature, while the areal proportion under precipitation dominance is projected to remain steady.

References

Abatzoglou, J.T., Brown, T.J., 2012. A comparison of statistical downscaling methods suited for wildfire applications. International Journal of Climatology, 32(5): 772-780.

Anderson, R.M., Koren, V.I., Reed, S.M., 2006. Using SSURGO data to improve Sacramento Model

Hydrol. Earth Syst. Sci. Discuss., doi:10.5194/hess-2016-493, 2016
Manuscript under review for journal Hydrol. Earth Syst. Sci.
Published: 5 October 2016

a priori parameter estimates. Journal of Hydrology, 320(1): 103-116.

Arnell, N.W., Gosling, S.N., 2013. The impacts of climate change on river flow regimes at the global scale. Journal of Hydrology, 486: 351-364.

Bae, D.-H., Jung, I.-W., Lettenmaier, D.P., 2011. Hydrologic uncertainties in climate change from IPCC AR4 GCM simulations of the Chungju Basin, Korea. Journal of Hydrology, 401(1): 90-105.

Barnett, T.P., Adam, J.C., Lettenmaier, D.P., 2005. Potential impacts of a warming climate on water availability in snow-dominated regions. Nature, 438(7066): 303-309.

Bosch, J.M., Hewlett, J., 1982. A review of catchment experiments to determine the effect of vegetation changes on water yield and evapotranspiration. Journal of hydrology, 55(1): 3-23.

Bosshard, T. et al., 2013. Quantifying uncertainty sources in an ensemble of hydrological climate - impact projections. Water Resources Research, 49(3): 1523-1536.

Burnash, R., 1995. The NWS river forecast system-catchment modeling. In: Singh, V. (Ed.), Computer models of watershed hydrology. Water Resources Publications, Littleton, Colorado, pp. 311-366.

Caldwell, P., Sun, G., McNulty, S., Cohen, E., Moore Myers, J., 2012. Impacts of impervious cover, water withdrawals, and climate change on river flows in the conterminous US. Hydrology and Earth System Sciences, 16(8): 2839-2857.

Challinor, A. et al., 2014. A meta-analysis of crop yield under climate change and adaptation. Nature Climate Change, 4: 287-291.

Chen, J., Brissette, F.P., Leconte, R., 2011. Uncertainty of downscaling method in quantifying the impact of climate change on hydrology. Journal of Hydrology, 401(3): 190-202.

Cheng, L. et al., 2014. Impacts of elevated CO 2, climate change and their interactions on water budgets in four different catchments in Australia. Journal of Hydrology, 519: 1350-1361.

Creed, I., Hwang, T., Lutz, B., Way, D., 2015. Climate warming causes intensification of the hydrological cycle, resulting in changes to the vernal and autumnal windows in a northern temperate forest. Hydrological Processes, 29(16): 3519-3534.

Dale, V.H. et al., 2001. Climate Change and Forest Disturbances Climate change can affect forests by altering the frequency, intensity, duration, and timing of fire, drought, introduced species, insect and pathogen outbreaks, hurricanes, windstorms, ice storms, or landslides. BioScience, 51(9): 723-734.

Daly, C. et al., 2008. Physiographically sensitive mapping of climatological temperature and precipitation across the conterminous United States. International Journal of Climatology, 28: 2031-2064.

Davis, J. et al., 2015. When trends intersect: The challenge of protecting freshwater ecosystems under multiple land use and hydrological intensification scenarios. Science of The Total Environment, 534: 65-78.

Duan, K., Mei, Y., 2014a. Comparison of Meteorological, Hydrological and Agricultural Drought Responses to Climate Change and Uncertainty Assessment. Water Resources Management, 28(14): 5039-5054.

Duan, K., Mei, Y., 2014b. A comparison study of three statistical downscaling methods and their model-averaging ensemble for precipitation downscaling in China. Theoretical and applied climatology, 116(3-4): 707-719.

Duan, K., Mei, Y., Zhang, L., 2016a. Copula-based bivariate flood frequency analysis in a changing climate—A case study in the Huai River Basin, China. Journal of Earth Science, 27(1): 37-46.

Duan, K. et al., 2016b. Divergence of ecosystem services in U.S. National Forests and Grasslands under a changing climate. Scientific Reports.

Ficklin, D.L., Luo, Y., Luedeling, E., Zhang, M., 2009. Climate change sensitivity assessment of a highly agricultural watershed using SWAT. Journal of Hydrology, 374(1): 16-29.

Gedney, N. et al., 2006. Detection of a direct carbon dioxide effect in continental river runoff records. Nature, 439(7078): 835-838.

Gibbons, J.D., Chakraborti, S., 2011. Nonparametric statistical inference. Springer, Berlin Heidelberg.

Giuntoli, I., Vidal, J.-P., Prudhomme, C., Hannah, D.M., 2015. Future hydrological extremes: the uncertainty from multiple global climate and global hydrological models. Earth System Dynamics, 6(1): 267-285.

Grant, G.E., Tague, C.L., Allen, C.D., 2013. Watering the forest for the trees: an emerging priority for managing water in forest landscapes. Frontiers in Ecology and the Environment, 11(6): 314-321.

Gupta, S.C., Kessler, A.C., Brown, M.K., Zvomuya, F., 2015. Climate and agricultural land use change impacts on streamflow in the upper midwestern United States. Water Resources Research, 51(7): 5301-5317.

IPCC, 2014. Climate Change 2014: Synthesis Report. Contribution of Working Groups I, II and III to the Fifth Assessment Report of the Intergovernmental Panel on Climate Change. 9291691437, IPCC, Geneva, Switzerland.

Jackson, R.B. et al., 2005. Trading water for carbon with biological carbon sequestration. Science, 310(5756): 1944-1947.

Jung, I.-W., Moradkhani, H., Chang, H., 2012. Uncertainty assessment of climate change impacts for hydrologically distinct river basins. Journal of Hydrology, 466: 73-87.

Karl, T.R., Riebsame, W.E., 1989. The impact of decadal fluctuations in mean precipitation and temperature on runoff: a sensitivity study over the United States. Climatic Change, 15(3): 423-447.

Kay, A., Davies, H., Bell, V., Jones, R., 2009. Comparison of uncertainty sources for climate change impacts: flood frequency in England. Climatic Change, 92(1-2): 41-63.

Koren, V., Smith, M., Duan, Q., 2003. Use of a priori parameter estimates in the derivation of spatially consistent parameter sets of rainfall‐runoff models. Calibration of Watershed Models. AGU, Washington, D.C., 239-254 pp.

Livneh, B. et al., 2013. A long-term hydrologically based dataset of land surface fluxes and states for the conterminous United States: update and extensions. Journal of Climate, 26(23): 9384-9392.

Lutz, A., Immerzeel, W., Shrestha, A., Bierkens, M., 2014. Consistent increase in High Asia's runoff due to increasing glacier melt and precipitation. Nature Climate Change, 4(7): 587-592.

Mauget, S.A., 2003. Multidecadal regime shifts in US streamflow, precipitation, and temperature at the end of the twentieth century. Journal of Climate, 16(23): 3905-3916.

McCabe, G.J., Markstrom, S.L., 2007. A monthly water-balance model driven by a graphical user interface. 2331-1258, Geological Survey (US).

McCabe, G.J., Wolock, D.M., 2002. A step increase in streamflow in the conterminous United States. Geophysical Research Letters, 29(24).

McCabe, G.J., Wolock, D.M., 2011. Independent effects of temperature and precipitation on modeled runoff in the conterminous United States. Water Resources Research, 47.

McCabe, G.J., Wolock, D.M., 2016. Variability and Trends in Runoff Efficiency in the Conterminous United States. Journal of the American Water Resources Association.

Mearns, L.O. et al., 2012. The North American regional climate change assessment program: overview of phase I results. Bulletin of the American Meteorological Society, 93(9): 1337-1362.

Milly, P., Dunne, K., 2016. Potential evapotranspiration and continental drying. Nature Climate Change.

Milly, P.C. et al., 2008. Stationarity is dead: Whither water management? Science, 319(5863): 573-574.

Milly, P.C., Dunne, K.A., Vecchia, A.V., 2005. Global pattern of trends in streamflow and water availability in a changing climate. Nature, 438(7066): 347-350.

Moss, R.H. et al., 2010. The next generation of scenarios for climate change research and assessment. Nature, 463(7282): 747-756.

Nash, L.L., Gleick, P.H., 1991. Sensitivity of streamflow in the Colorado basin to climatic changes. Journal of hydrology, 125(3): 221-241.

Piao, S. et al., 2010. The impacts of climate change on water resources and agriculture in China. Nature, 467(7311): 43-51.

Ryberg, K.R., Lin, W., Vecchia, A.V., 2014. Impact of climate variability on runoff in the North-Central United States. Journal of Hydrologic Engineering, 19(1): 148-158.

Schewe, J. et al., 2014. Multimodel assessment of water scarcity under climate change. Proceedings of the National Academy of Sciences, 111(9): 3245-3250.

Seager, R. et al., 2013. Projections of declining surface-water availability for the southwestern United States. Nature Climate Change, 3(5): 482-486.

Sun, G. et al., 2011a. A general predictive model for estimating monthly ecosystem evapotranspiration. Ecohydrology, 4(2): 245-255.

Sun, G. et al., 2011b. Upscaling key ecosystem functions across the conterminous United States by a water - centric ecosystem model. Journal of Geophysical Research, 116.

Sun, G., Caldwell, P.V., McNulty, S.G., 2015a. Modelling the potential role of forest thinning in maintaining water supplies under a changing climate across the conterminous United States. Hydrological Processes, 29(24): 5016-5030.

Sun, S. et al., 2015b. Drought impacts on ecosystem functions of the US National Forests and Grasslands: Part I evaluation of a water and carbon balance model. Forest Ecology and Management, 353: 260-268.

Teixeira, E.I., Fischer, G., van Velthuizen, H., Walter, C., Ewert, F., 2013. Global hot-spots of heat stress on agricultural crops due to climate change. Agricultural and Forest Meteorology, 170: 206-215.

Trenberth, K.E. et al., 2014. Global warming and changes in drought. Nature Climate Change, 4(1): 17-22.

Vörösmarty, C.J., Green, P., Salisbury, J., Lammers, R.B., 2000. Global water resources: vulnerability from climate change and population growth. science, 289(5477): 284-288.

Vano, J.A., Das, T., Lettenmaier, D.P., 2012. Hydrologic sensitivities of Colorado River runoff to changes in precipitation and temperature*. Journal of Hydrometeorology, 13(3): 932-949.

Vose, J.M. et al., 2016. Ecohydrological implications of drought for forests in the United States. Forest Ecology and Management.

Wilby, R.L., Harris, I., 2006. A framework for assessing uncertainties in climate change impacts: Low‐flow scenarios for the River Thames, UK. Water Resources Research, 42(2).

Woodhouse, C.A., Pederson, G.T., Morino, K., McAfee, S.A., McCabe, G.J., 2016. Increasing influence of air temperature on upper Colorado River streamflow. Geophysical Research Letters, 43(5): 2174-2181.

Zhang, D., Cong, Z., Ni, G., Yang, D., Hu, S., 2015. Effects of snow ratio on annual runoff within the Budyko framework. Hydrology and Earth System Sciences, 19(4): 1977-1992.

Zhang, L., Dawes, W., Walker, G., 2001. Response of mean annual evapotranspiration to vegetation changes at catchment scale. Water resources research, 37(3): 701-708.

Zhou, G. et al., 2015. Global pattern for the effect of climate and land cover on water yield. Nature communications, 6.

Data availability

All data used in the analysis and conclusions in this paper are available in the references.

Acknowledgements

This work was supported by the National Science Foundation EaSM program (AGS-1049200) awarded to North Carolina State University, and the Eastern Forest Environmental Threat Assessment Center (EFETAC), USDA Forest Service, Raleigh, NC. The MACAv2-LIVNEH dataset was produced under the Northwest Climate Science Center (NW CSC) US Geological Survey Grant Number

Hydrol. Earth Syst. Sci. Discuss., doi:10.5194/hess-2016-493, 2016
Manuscript under review for journal Hydrol. Earth Syst. Sci.
Published: 5 October 2016

G12AC20495. Partial support was provided by the Natural Science Foundation of Jiangsu Province, China (BK20151525); the Pine Integrated Network: Education, Mitigation, and Adaptation project (PINEMAP), which is a Coordinated Agricultural Project funded by the USDA National Institute of Food and Agriculture, Award #2011-68002-30185. All data used in the analysis and conclusions in this paper are available in the references or supporting information.

Hydrol. Earth Syst. Sci. Discuss., doi:10.5194/hess-2016-493, 2016
Manuscript under review for journal Hydrol. Earth Syst. Sci.
Published: 5 October 2016

Hydrology and Earth System Sciences
Open Access
Discussions

Tables

Table 1. Average changes in mean annual precipitation and temperature over the entire CONUS from the baseline scenario (B) to future scenarios (S1~S4)

GCM	Country	Precipitation (mm yr^{-1})					Temperature (°C)				
		B	S1	S2	S3	S4	B	S1	S2	S3	S4
bcc-csm1-1	China	787	-3	+13	+33	-5	11.4	+1.7	+2.4	+1.9	+4.8
bcc-csm1-1-m	China	786	+18	-18	+29	+33	11.4	+1.5	+2.4	+1.7	+4.3
BNU-ESM	China	798	+51	+42	+25	+45	11.5	+1.9	+3.2	+2.0	+5.4
CanESM2	Canada	800	+14	+42	+19	+83	11.3	+2.3	+3.5	+2.4	+5.8
CCSM4	USA	783	+29	+29	+18	+58	11.5	+1.5	+2.5	+1.9	+4.6
CNRM-CM5	France	780	+46	+56	+40	+85	11.4	+1.4	+2.8	+1.6	+4.6
CSIRO-Mk3-6-0	Australia	780	+14	+84	+24	+74	11.2	+2.0	+3.4	+2.0	+5.6
GFDL-ESM2M	USA	787	+6	+20	+32	+31	11.3	+1.6	+2.2	+1.7	+4.2
GFDL-ESM2G	USA	791	+21	+36	+38	+12	11.4	+1.2	+1.7	+1.2	+3.7
HadGEM2-ES	UK	784	+16	+7	+18	+7	11.3	+2.2	+3.8	+2.5	+6.8
HadGEM2-CC	UK	779	+23	+39	+5	+32	11.3	+2.3	+4.2	+2.7	+6.7
inmcm4	Russia	779	-7	+4	+0	+13	11.4	+0.9	+1.7	+1.1	+3.4
IPSL-CM5A-LR	France	780	+8	+14	+13	-8	11.5	+1.8	+3.0	+1.8	+5.8
IPSL-CM5A-MR	France	789	-4	+13	-25	-70	11.3	+1.9	+3.2	+2.3	+6.0
IPSL-CM5B-LR	France	781	+23	+62	+34	+82	11.4	+1.5	+2.4	+1.7	+4.4
MIROC5	Japan	788	+9	+10	+24	+6	11.2	+2.3	+3.6	+2.4	+5.7
MIROC-ESM	Japan	791	+56	+37	+30	+9	11.3	+2.1	+4.1	+2.6	+6.6
MIROC-ESM-CHEM	Japan	784	+12	+38	+26	+10	11.4	+2.4	+4.0	+2.7	+6.9
MRI-CGCM3	Japan	783	+20	+47	+38	+87	11.4	+0.8	+1.7	+1.0	+3.2
NorESM1-M	Norway	784	+13	+31	+25	+63	11.3	+1.8	+3.1	+2.2	+5.1

Hydrol. Earth Syst. Sci. Discuss., doi:10.5194/hess-2016-493, 2016
Manuscript under review for journal Hydrol. Earth Syst. Sci.
Published: 5 October 2016

Hydrology and Earth System Sciences
Discussions
Open Access

Table 2. Comparison of multi-model averaged contributions (%) of precipitation (*P*), temperature (*T*), and interactions between *P* and *T* (*P&T*) to changes in runoff in the 18 WRRs in historical period (1961-2010) and future scenarios (S1~S4).

WRR	Historical			S1				S2				S3				S4			
	P	*T*	*P&T*	*P*	*T*	*P&T*	Sig[b]	*P*	*T*	*P&T*	Sig	*P*	*T*	*P&T*	Sig	*P*	*T*	*P&T*	Sig
1	**99.97**[a]	0.01	0.01	**55**	44	1	√	**52**	47	1	×	**53**	46	1	×	48	**51**	2	×
2	**99.92**	0.04	0.04	45	**53**	2	×	46	**52**	1	×	47	**51**	2	×	43	**55**	2	√
3	**99.98**	0.01	0.01	43	**49**	8	×	39	**55**	5	√	42	**51**	7	×	33	**60**	8	√
4	**99.91**	0.05	0.05	41	**58**	1	×	38	**60**	1	√	46	**53**	1	×	36	**62**	2	√
5	**99.91**	0.04	0.04	38	**60**	3	√	36	**61**	2	√	43	**54**	2	×	36	**62**	3	√
6	**99.98**	0.01	0.01	40	**56**	4	×	40	**57**	3	√	46	**51**	4	×	36	**59**	4	√
7	**99.85**	0.07	0.07	36	**62**	2	√	31	**67**	2	√	35	**62**	3	√	30	**67**	3	√
8	**99.77**	0.12	0.12	38	**53**	9	×	33	**59**	8	√	35	**56**	9	√	29	**61**	10	√
9	**100.0**	0.00	0.00	35	**60**	5	√	31	**64**	5	√	38	**57**	5	√	30	**60**	9	√
10	**99.90**	0.05	0.05	31	**61**	8	√	30	**63**	7	√	30	**63**	7	√	31	**61**	8	√
11	**99.96**	0.02	0.02	30	**55**	15	√	27	**62**	11	√	27	**59**	15	√	26	**64**	10	√
12	**99.94**	0.03	0.03	**45**	38	17	×	37	**46**	17	×	38	**43**	19	×	31	**52**	17	√
13	**99.92**	0.04	0.04	37	**52**	11	×	37	**55**	7	√	36	**54**	10	√	26	**64**	10	√
14	**99.93**	0.03	0.03	33	**62**	5	√	35	**60**	4	√	31	**66**	3	√	31	**63**	7	√
15	**99.89**	0.06	0.06	38	**53**	9	×	42	**48**	10	×	41	**52**	7	×	37	**50**	13	×
16	**99.99**	0.00	0.00	30	**65**	5	√	32	**61**	7	√	29	**64**	6	√	33	**56**	11	√
17	**99.95**	0.02	0.02	38	**60**	2	×	38	**60**	2	√	38	**59**	2	√	39	**58**	3	√
18	**99.85**	0.08	0.08	**56**	40	3	×	**50**	46	4	×	**54**	44	2	×	**52**	44	4	×
CONUS	**99.92**	0.04	0.04	33	**61**	6	√	35	**62**	3	√	38	**58**	4	√	31	**65**	4	√

[a]The largest contributor among the three factors is underlined and bolded.

[b]Significance of the Wilcoxon signed-rank test for the differences between the contributions of *P* and *T* at 5% significance level. The hypothesis is that the differences projected from the 20 GCMs come from a distribution with zero median. " √ " and "×" indicate that the difference is significant and insignificant, respectively.

Hydrol. Earth Syst. Sci. Discuss., doi:10.5194/hess-2016-493, 2016
Manuscript under review for journal Hydrol. Earth Syst. Sci.
Published: 5 October 2016

Table 3. Cross comparison of the areal proportions (%) with different dominant driving factors and changes directions of runoff in the future scenarios (S1~S4).

Scenario	S1	S2	S3	S4
P-dominant				
R↗ [a]	12	12	12	11
R↘	0	0	0	0
Total	12	12	12	11
T-dominant				
R↗	1	0	1	0
R↘	36	46	33	52
Total	36	47	34	52
Non-dominant (*MCP* > *MCT*)				
R↗	10	10	11	7
R↘	2	5	3	9
Total	12	15	13	16
Non-dominant (*MCT* > *MCP*)				
R↗	3	2	3	0
R↘	36	23	37	20
Total	40	26	41	20

[a] "↗" and "↘" indicate increase and decrease in the multi-model means of runoff, respectively.

Hydrol. Earth Syst. Sci. Discuss., doi:10.5194/hess-2016-493, 2016
Manuscript under review for journal Hydrol. Earth Syst. Sci.
Published: 5 October 2016

Hydrology and Earth System Sciences
Open Access
Discussions

Figures

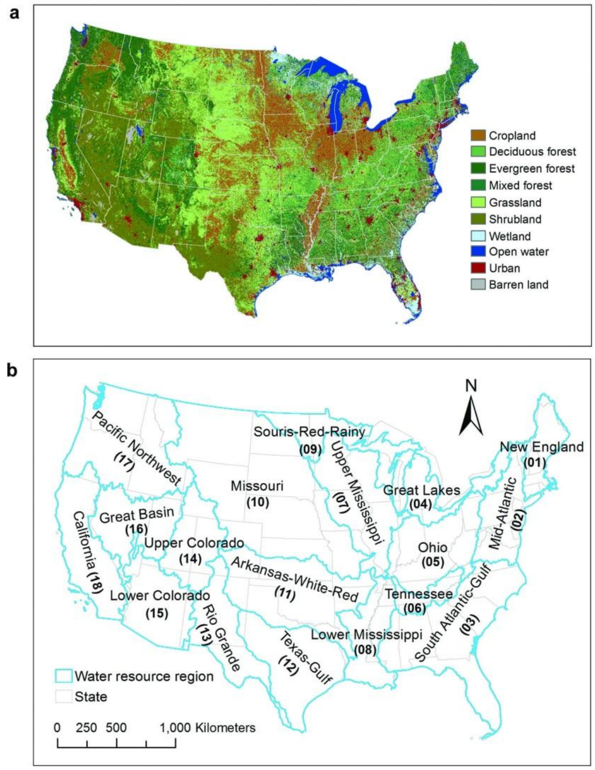

Figure 1. (**a**) Land-cover distribution in the CONUS from the 2006 National Land Cover Database (http://www.mrlc.gov/nlcd06_data.php), and (**b**) location of the 18 Water Resource Regions (WRRs).

Hydrol. Earth Syst. Sci. Discuss., doi:10.5194/hess-2016-493, 2016
Manuscript under review for journal Hydrol. Earth Syst. Sci.
Published: 5 October 2016

Hydrology and Earth System Sciences
Discussions
Open Access

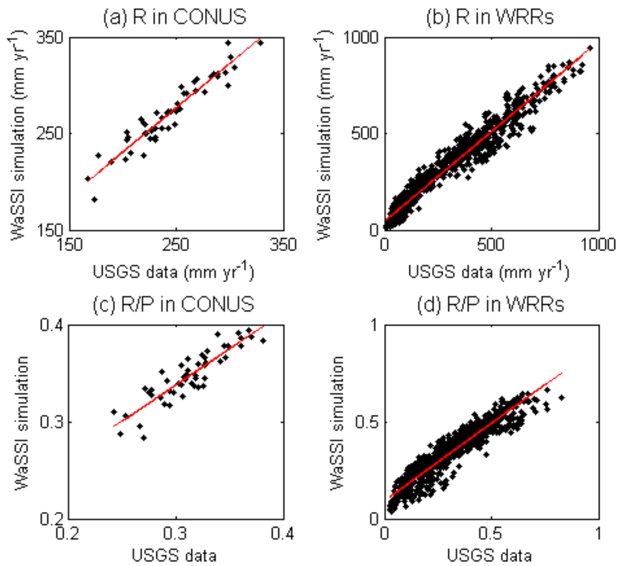

Figure 2. Validations of the WaSSI model at the CONUS and WRR levels. **a-b**, Comparisons of simulated annual runoff (mm yr^{-1}) against USGS observed data in 1961-2010 over the entire CONUS (**a**) and in 18 WRRs (**b**). **c-d**, Comparisons of simulated runoff coefficient (runoff / precipitation, R/P) against that derived from USGS observed data in the CONUS (**c**) and WRRs (**d**).

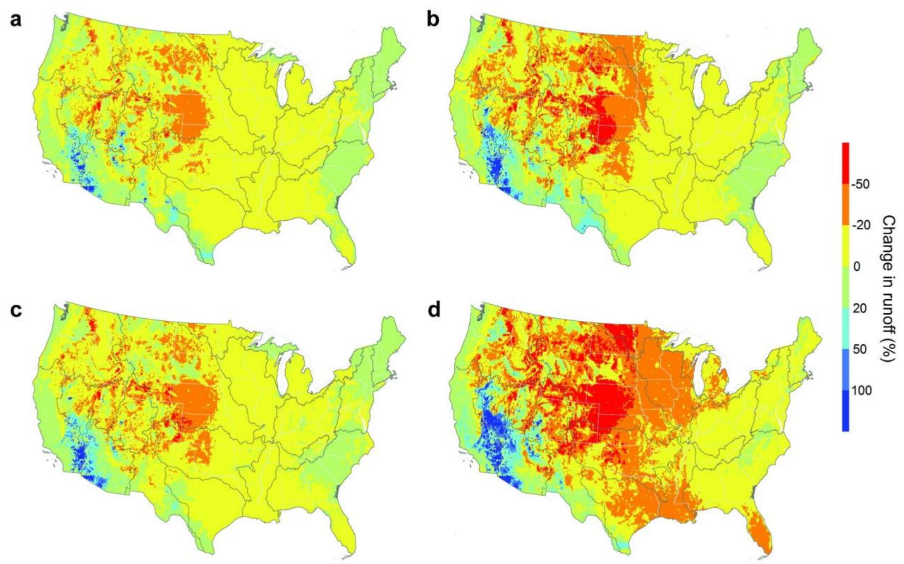

Figure 3. Projected changes in multi-year mean annual runoff (%) across the CONUS. **a-d**, Changes from the baseline to S1 (RCP4.5/2030s) (**a**), S2 (RCP4.5/2080s) (**b**), S3 (RCP8.5/2030s) (**c**), and S4 (RCP8.5/2080s) (**d**) scenarios. The maps display the multi-model mean changes from the 20 GCMs in each HUC-12 watershed across the CONUS.

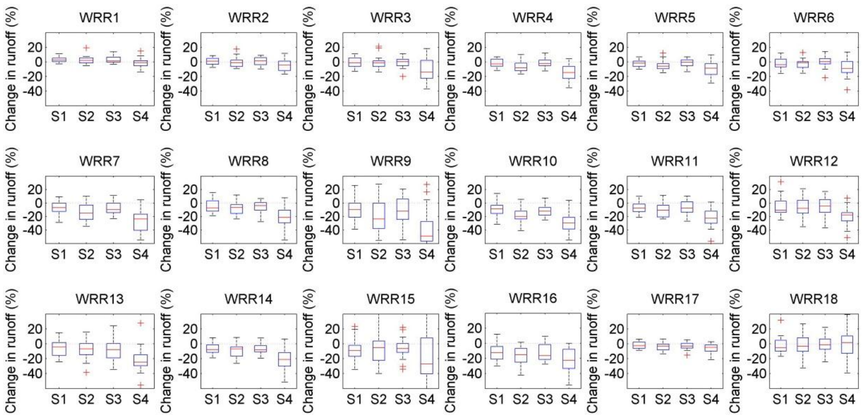

Figure 4. Area-averaged changes in runoff in the 18 WRRs in the future scenarios. The four future scenarios are denoted by S1 (RCP4.5/2030s), S2 (RCP4.5/2080s), S3 (RCP8.5/2030s), and S4 (RCP8.5/2080s) in the x-axis. The vertical spread of the box-whisker plots shows the different results projected from the 20 GCMs, with the boxes covering the ranges from 25% quartile to 75% quartile of the distributions (Inter-Quartile Range, IQR) and the red lines within each box marking the median values. Points outside the whiskers are taken as extreme outliers and marked by plus signs.

Hydrology and Earth System Sciences
Discussions
Open Access

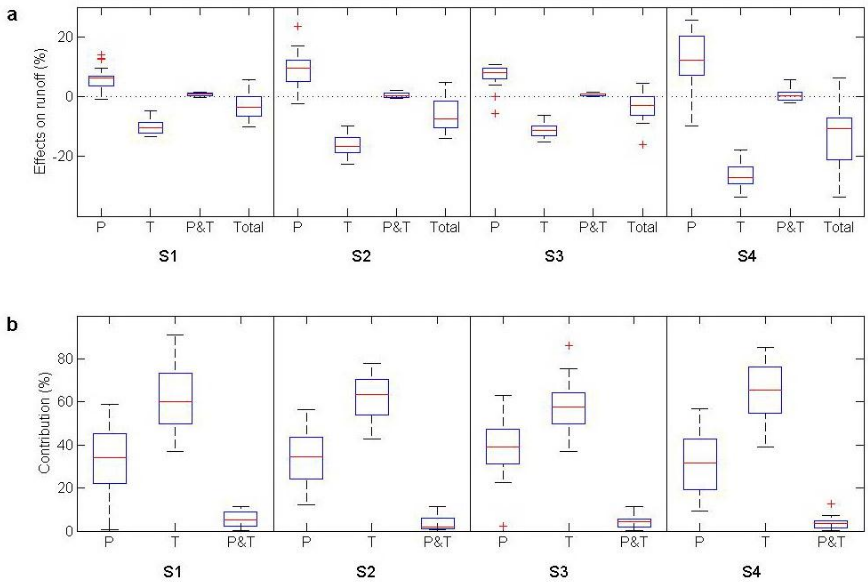

Figure 5. Effects of P, T, and $P\&T$ on annual runoff over the entire CONUS. **a**, Independent effects of P, T, and $P\&T$ on runoff, and their sum (Total) in the future scenarios. **b**, Contributions of P, T, and $P\&T$ to runoff changes in the future scenarios.

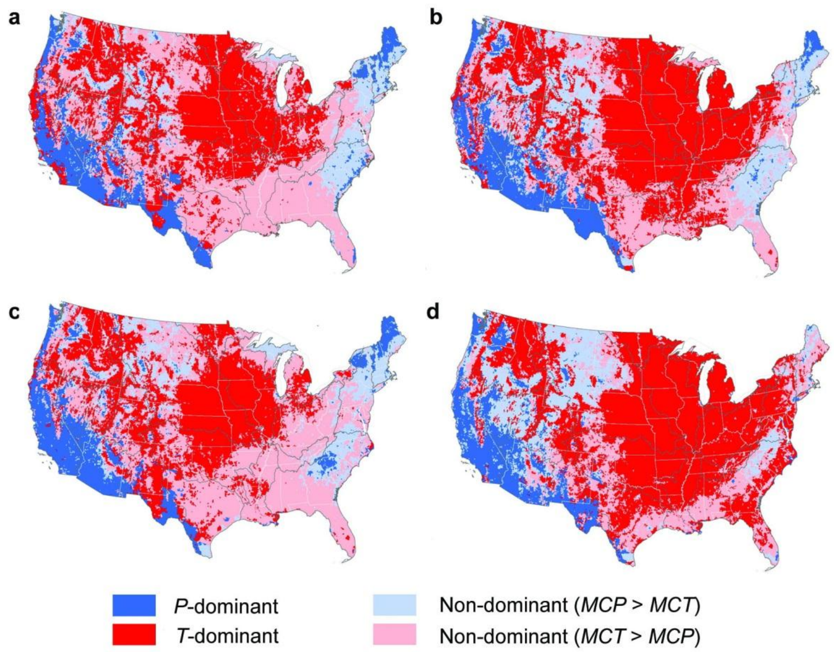

Figure 6. Dominant drivers of runoff change in the CONUS. **a-d**, Distribution of precipitation-change-dominant (*P*-dominant), temperature-change-dominant (*T*-dominant), and non-dominant (*MCP* > *MCT* or *MCT* > *MCP*) HUC-12 watersheds across the CONUS in S1 (RCP4.5/2030s) (**a**), S2 (RCP4.5/2080s) (**b**), S3 (RCP8.5/2030s) (**c**), and S4 (RCP8.5/2080s) (**d**) scenarios. The results displayed in the maps are derived from the multi-model means of the 20 GCMs.